Gut-Germline Axis:
A Reproductive Endosymbiont's Adaptation
is Modulated by the Gut Microbiome

Madangchanok Imchen[1], Rupinder Kaur[1], Darlene Huilin Zhou Luo[1], Mia W. Bitman[1], Emilie Lefoulon[1], Angelina McGarry[1], Sarah R. Bordenstein, and Seth R. Bordenstein[1]*

[1]Departments of Biology and Entomology, One Heath Microbiome Center, Huck Institutes of the Life Sciences, The Pennsylvania State University, USA

*Corresponding author: srb6251@psu.edu

Keywords: cytoplasmic incompatibility, microbiome, intracellular bacteria, endosymbiosis, *Drosophila melanogaster*

Abstract

Holobionts contain extra- and intracellular microbes that are typically studied in symbiotic and anatomical siloes. Here we demonstrate a previously unknown impact of the extracellular gut microbiome on the adaptation of a reproductive endosymbiont. Specifically, a paternal-effect embryonic lethality caused by *Wolbachia*-induced cytoplasmic incompatibility (CI) is attenuated by the gut microbiome. Gut microbiome-mediated variation in the CI phenotype causes key gene expression changes in the symbiosis and defining cell biological defects in the evolutionary conserved histone-to-protamine transition that drives CI. Reintroducing the gut microbiome into germ-free flies recapitulates the CI attenuation. Notably, the integrated holobiont exhibits significantly elevated gut microbiome and endosymbiont densities relative to isolated constituent rearing, highlighting a synergistic relationship. Finally, impacts of the symbionts on survival are independent and inversely related throughout development, and fitness changes are recapitulated when the gut microbiome is restored. Altogether, this study uncovers a gut-germline axis in which bacteria shape an entangled network of symbiotic functions within a holobiont. Interorgan, symbiotic relationships have far-reaching implications for the study of trait variation.

Main

Animal and plant holobionts harbor consortia of microorganisms, encompassing endosymbionts and extracellular microbes with varying degrees of interdependencies[1–3]. The co-existence of these microbial classes with different lifestyles and functions can hypothetically exert influences in competitive, collaborative, or stochastic ways[4]. If such trade-offs and synergies occur across diverse symbiotic types and host anatomical sites, then they can drive cascading, ripple effects of symbiosis throughout the entire holobiont. However, such effects have not been a focal point of study owing to two primary factors. First, conventional microbiome elimination methods are indiscriminate, affecting both symbiont classes. Second, the obligatory intracellular nature of endosymbionts often precludes their cultivation[5]. Here, we overcome these limitations in a system that contains a vertically-inherited, intracellular endosymbiont and an environmentally-acquired gut microbiome.

In the *Drosophila melanogaster* holobiont, the α-proteobacterium *Wolbachia* is an archetypal reproductive endosymbiont of *D. melanogaster* and one of the most prevalent maternally-inherited bacteria in animals[6]. The endosymbiont is widely known for replication in the reproductive tract and diverse manipulations of arthropod reproductive biology. The most common adaptation that *Wolbachia* deploy is cytoplasmic incompatibility (CI), a phenomenon in which crosses between symbiotic males and aposymbiotic females result in embryonic lethality[7–11]. Embryos are rescued if the females harbor *Wolbachia*. Consequently, CI selfishly enhances the relative fitness of symbiont-transmitting females, thereby spreading *Wolbachia*[8]. In addition, a combined body of evidence specifies that *D. melanogaster* houses a simple and beneficial gut microbiome of a handful of core species that can be easily removed[12]. *Wolbachia* are absent from the *D. melanogaster* gut lumen[13], suggesting there is no obvious route for an interaction with its

simple gut microbiome. However, indirect associations occur wherein *Wolbachia* associate with gut microbiome composition[13,14].

The last decade of work in host-microbial interactions has featured a large increase in functional studies of binary symbioses or experimental studies of single anatomical sites of symbiotic interactions. This wave of experiments has inspired a good deal of new conceptual and theoretical work on the complexity of holobionts that house a rich aggregate of microbes across the body. Here we address three fundamental questions to unravel symbiotic functions in a holobiont context: (i) Can a reproductive endosymbiont (*Wolbachia*) function autonomously of the gut microbiome? (ii) What effects does the gut microbiome have on densities, penetrance, gene expression, and cell biological underpinnings of the endosymbiont? And (iii) How is host fitness independently and synergistically shaped by the gut and reproductive microbiome? By tackling these inquiries, this study reveals an overlooked, functional interplay between bacteria in different host organs and their combined influence on holobiont biology.

Results

We generated *D. melanogaster* with and without *Wolbachia* and the gut microbiome by leveraging dechorionation of the fertilized eggshell layer in *Drosophila melanogaster*, a process that eliminates the extracellular gut microbiome[12] while preserving the vertically-inherited, reproductive endosymbiont. For simplicity and the purposes of the paper, we separately define the conventional microbiome as the community of gut microbes. Thus, we adhere to the typical nomenclature of conventional (CV) and germ-free (GF) hosts, both with *Wolbachia* (CV+ and GF+) and without it (CV- and GF-) (Fig 1A). We confirmed *Wolbachia* infection status by PCR and GF status by plating whole fly homogenates (see methods) to detect the presence/absence of

colony-forming units (CFUs) (Fig S1). We also confirmed that the CV+/- lines have the same genetic makeup (Table S1).

The adaptation and host regulation of a reproductive endosymbiont are altered by the gut microbiome

If the *Wolbachia* reproductive endosymbionts in the reproductive tissue are modulated by the presence of a gut microbiome, then we expect that CI will increase or decrease in the absence of a gut microbiome. To test this prediction, we mated CI-inducing males with *Wolbachia* (CV+ and GF+) and aposymbiotic females without *Wolbachia* (CV-) in single, pairwise matings. All males in these CI assays were <1-day-old since they cause a strong CI lethality[15], which is measured as a percent reduction of embryonic hatching into larvae. In multiple experiments, GF+ males induced 2.6-fold stronger CI (median embryonic hatch rate = 13.66%) relative to CV+ males (median = 36.17%) (Fig 1B). This increase in embryonic lethality was fully rescued by CV+ females, confirming the effect is bona fide CI rather than artifactual host sterility. These results specify that *Wolbachia* can alone induce CI and the penetrance of the trait is attenuated by the presence of the gut microbiome. To validate this interpretation, we conducted a microbiome transplant experiment into GF+ males via fecal-oral transmission. Restoration of the CV+ native microbiome likewise attenuated the enhanced CI penetrance (Fig 1C). Thus, the enhanced CI penetrance in GF+ was reversible with a 4.72-fold decrease that matched that of CV+ CI (Fig 1C), demonstrating the gut microbiome's causal role in modulating CI-*Wolbachia*.

Given that *Wolbachia* initiate CI with nucleoprotein modifications in developing sperm[7,16], we next reasoned that the fly transcriptome could be a sensitive measure of host

regulatory changes in GF+ vs. CV+ males. Indeed, expression analyses revealed changes to CI-defining gametic modifications in the histone-to-protamine transition in late male pupae, which is when this protein transition begins in *D. melanogaster*[17,18]. The core nucleosome structure is composed of histone classes H2A, H2B, H3, and H4[19], and expression of the *His2Av*, *His2B*, *His3.3A*, *His3.3B*, and *His4r* genes were upregulated in GF+ pupae that induce stronger CI compared to CV+ (Fig 1D; Table S2). In total, expression of 8 out of 10 histone associated genes were more elevated in GF+/CV+ compared to GF-/CV-. These results are consistent with the increased histone retention of CI sperm[7]. In *Drosophila* spermiogenesis, the histone variant *H3.3* along with the bulk histones are removed in the early canoe stage during the protein transition[20]. Expression of the *His3.3B* gene encoding the H3.3 histone protein[21] was significantly upregulated in GF+ males relative to CV+ males (fold change = 1.84, Log2FC= 0.88 $p < 0.05$). Moreover, expression of histone methyltransferase 4-20 (*Hmt4-20*) that marks DNA for damage repair[22] was also significantly upregulated (fold change = 1.83, Log2FC= 0.87), which is consistent with the fly quiescing elevated DNA damage also known to occur in developing CI sperm[23]. Consequently, *Wolbachia* enhance gene expression of histone-related CI features in the GF+ state.

There are four well-characterized protamine and protamine-like genes essential for *Drosophila* mature sperm formation[24,25]. Consistent with CI's causal role in depleting protamine abundance in sperm[7,16], *ProtB*, *Prtl99C*, and *Mst77F* were significantly downregulated in GF+ vs. CV+ male pupae (Fig 1C), and *ProtA* expression trended lower (Table S2). Three out of the four significant protamine genes expressed lower transcription in GF+/CV+ relative to GF-/CV-. Moreover, 13 of the 15 significant male-specific transcript (*Mst*) genes, involved in secretory proteins and spermatid maturation, e.g., *Mst57Da*, *Mst57Db*, and *Mst57Dc*, had a more

pronounced change in GF+/CV+ relative to GF-/CV-. Thus, *Wolbachia* generally weaken gene expression of these sperm-associated proteins. Collectively, results show that transcriptomic alterations in key CI cellular pathway genes link to the augmented CI penetrance in gut microbiome-deficient flies.

Finally, analysis of the top 25 differentially-expressed host transcripts between GF vs CV flies revealed gene expression changes associated with male accessory gland proteins that are transferred to females during mating (*Mst57Da*, CG9997, and CG9029) (Fig S2). There were also transcripts involved in chitin-based cuticle development, cuticle and trachea development[26], light-sensitive photoreceptor rhodopsins, and unannotated markers. Taken together, the results imply that GF+ flies are transcriptionally altered in diverse ways, with mechanistic relevance to *Wolbachia* pathology and the acute sperm development changes that underpin CI.

Endosymbiont-driven sperm chromatin remodeling is sensitive to the gut microbiome

Based on the sperm-associated regulatory changes above, we next leveraged cell biological markers of chromatin integrity to test if CI-nucleoprotein signatures increase in GF+ flies during the critical sperm developmental stages when the histone-to-protamine transition takes place (Fig 2A). We first examined the total histone levels in GF+ spermatids using a core histone antibody and show histone retention in both GF+ and CV+ males in late canoe spermatid bundles compared to GF- and CV-, respectively. The level of histone retention between the two groups varied, with GF+ canoe spermatids exhibiting a median of 15.48% histone retention compared to 0% for GF- males (Fig 2B), and CV+ testes showing 57.14% histone retention

compared to 12.14% for CV- males. As such, quantitative differences in histone retention are enhanced in CV+ males, while qualitative differences are greater in GF+ males.

Chromomycin A3 (CMA3) stain binds DNA regions devoid of protamines and assays if CI sperm experience protamine deficiency. Cytochemical staining of mature sperm from <1-day-old virgin males showed that protamine deficiency is 1.45-fold elevated in mature sperm of GF+ compared to GF- males (Fig 2C), which is slightly larger than the 1.3-fold difference in CV+ vs. CV- males (Fig 2C). Taken together, these results link CI variation and the transcriptome changes to sperm integrity changes *in situ*, namely that *Wolbachia* in a GF+ host enhance several central dogma underpinnings of CI. Our previous genetic work demonstrated that enhanced protamine deficiency is causal to increases in CI penetrance[23].

The gut microbiome lowers densities and transcriptional activity of the endosymbiont

CI strength varies with densities of *Wolbachia*[27], expression of the *cifA* and *cifB* genes[28], host genetic effects, among other facrtors[29]. To examine the impacts of the gut microbiome on *Wolbachia* densities, we quantified relative *Wolbachia* counts (*groEL)* normalized to *D. melanogaster* housekeeping gene *rp49*. Unexpectedly, *Wolbachia* density was reduced 2.07-fold ($p<0.05$) in strong CI-inducing GF+ males compared to CV+ males, but not in larvae (Fig 3A,B and S3). Furthermore, the relative gene expression of *cifA* and *cifB* compared to *Wolbachia groEL* was similar between CV+ and GF+ in adults (Fig 3C,D) and larvae (Fig 3E,F), indicating that *cif* transcription is independent of the *Wolbachia* density decline and loss of the extracellular

microbiome. These findings indicate that an intact CV+ fly holobiont has higher *Wolbachia* copies than a GF+ fly with *Wolbachia*, and the enhanced CI in GF+ males is surprisingly not attributable to increased symbiont abundance or CI gene expression. Since there were no expression changes to the CI genes, we investigated *Wolbachia* transcriptome variation by analyzing *Wolbachia* reads in the gene expression dataset above across embryos, larvae, male pupae, and male adults. During the larval stage when the testes develop in flies and both the spermatogonia and spermatocytes take form and store RNA transcripts for remodeling sperm development, *Wolbachia* in GF+ significantly overexpress ribosomal RNAs and mRNAs relative to CV+. The highest number of annotated *Wolbachia* functions includes host-microbe interactions, secretion system and virulence effectors, as well as ankyrin-containing proteins widely involved in host-microbe relationships (Fig 3G, blue category). Changes in protein synthesis transcripts and membrane transport further support that *Wolbachia* are transcriptionally altered in GF+ larvae to hypermodify host biology.

Finally, the microbiome of *D. melanogaster* is predominantly composed of 5 core culturable species from the genera *Lactobacillus* and *Acetobacter*[12]. To assess if *Wolbachia* also have a reverse impact on gut bacterial abundance between CV+ and CV- flies, we plated whole adult male homogenates onto *Lactobacillus* (MRS agar plates) and *Acetobacter* spp. (MYPL agar plates) selective media[30] and counted the number of colony forming units (CFUs) after 48 hours (Fig 4A). CFUs of *Acetobacter* and *Lactobacillus* species in CV+ were notably 7.07- and 9.78-fold higher compared to CV- (Fig 4B). Thus, an intact holobiont with the endosymbiont contains nearly an order of magnitude more cells of the extracellular microbiome. Moreover, there was a positive correlation between the overall CFUs of *Acetobacter* and *Lactobacillus* (Fig 4C) that validated previous reports[31,32]. In parallel, we demonstrated no CFUs from negative-

control homogenates from GF+ and GF- males, as expected (Fig S1). Taken together with data in Fig 3, the intact holobiont contains markedly more cells of both the extracellular gut microbiome and *Wolbachia* endosymbiont.

The gut microbiome and endosymbiont independently impact survival across development

By disentangling the gut microbiome and endosymbiont into constituent parts relative to the intact holobiont, we tested how the gut microbiome and *Wolbachia* differentially impact host fitness (survival) across metamorphosis. GF+ flies had a significantly higher embryonic hatch rate to larvae (71.43%) than GF- flies without *Wolbachia* (66.95%, Fig 5A). CV+ flies similarly also had higher embryo-to-larvae survival (87%) than CV- flies lacking *Wolbachia* (82%). Thus, the presence of *Wolbachia* modestly enhanced early life survivability. Moreover, CV+ embryos with higher *Wolbachia* counts also exhibited higher embryo-to-larval hatching (87%) than GF+ (71.43%), indicating that the complete microbiome and/or its possible impacts on an increase in *Wolbachia* density are beneficial for embryo-to-larvae survivability. From larval-to-pupal (L-P) and pupal-to-adult (P-A) development stages, *Wolbachia* generally reduced CV and GF host survival compared to their negative control counterparts, specifying a modest, negative fitness cost at the larval stage onwards (4-13% reduction in survival, Fig 5B,C). Nonetheless, holobiont survival was higher during the L-P stage (CV+ vs GF+, 11.67% increase, Fig 5B), indicating a compensatory effect of the extracellular microbiome. Overall, GF+ embryo-to-adult survival (38.56%) was noticeably lower than CV+ survival (51.56%) (Fig 5D), which was causally compensated upon microbiome reintroduction into GF+ (GF_M+ egg-to-adult survival = 51.35%)

(Figure 5E). Altogether, these findings specify independent impacts of the symbiont classes on survival across development, namely *Wolbachia* are beneficial to embryonic-to-larval development and harmful to subsequent stages, while the gut microbiome increases embryo-to-larval and larval-to-pupal survival during metamorphosis. Such effects can shape host fitness and will depend on genetic variation of both the host[33] and the endosymbiont.

Discussion

Holobionts are units in biology's hierarchy of organization that encompass the host organism and its associated microbial communities[3], including both intracellular (endosymbionts) and extracellular microbes. The interwoven existence of these distinct microbial groups spanning different anatomical locations, each with unique lifestyles and functional roles, is recognized after decades of study but rarely studied in a functional context. Here we addressed this knowledge gap by examining the adaptation, densities, transcriptomes, host modifications, and fitness impacts of a reproductive endosymbiont in the presence and absence of a gut microbiome. The accumulated lines of evidence add an unexpected dimension of the causes of variation that affect intimate, host-microbial symbioses.

We report five main findings: (i) CI penetrance is heightened in a host without a gut microbiome. (ii) Transplantation of the gut microbiome by fecal ingestion into a germ-free host causes the reduced CI penetrance. (iii) Host gene expression and cell biological hallmarks in the histone-to-protamine transition of sperm development underpin CI variation in germ-free vs. conventional hosts[7,23]. (iv) *Wolbachia* gene expression shows host interactions are linked to the heightened CI effect. (v) Intact holobionts have markedly higher microbial densities of both the

endosymbiont and gut microbiome relative to when one microbial class is missing, suggesting synergies on their within-host fitness.

The study of within-host symbiotic dynamics, especially across organs, remains in its infancy. Not surprisingly, much of the history of studying host-microbe interactions has emphasized simple, binary, host-microbe interactions or single, anatomical sites in the case of the host-associated microbial communities. Consequently, assumptions prevail that the causes of functional variation in host-microbe interactions are due to genetic and environmental variation of the interacting partners. Indeed, CI penetrance in various arthropods can vary with endosymbiont density, *cif* gene expression, host age, and host genetic background[34–43]. This broad assumption is now questionable in light of the complexity of holobiont systems with varying numbers and types of microorganisms across body sites that can affect the cell biology and physiology of the host. In mosquitoes, the gut bacterial genus *Asaia* can impede the vertical transmission of *Wolbachia*[44]. As such, nested symbiotic interactions between symbionts in different anatomical sites raise a fresh perspective and suite of questions on how one microbial class impacts the functions of another across the biogeography of the body. If these effects are widespread as we suspect, it might also aid explanations of the missing heritability problem in symbioses in which host genetic variation insufficiently explains variation in microbial traits.

In conclusion, this work disentangles the intricate relationship of the gut microbiome's impact on a key adaptation and replication of a common reproductive endosymbiont. It aligns with the growing recognition that sources of phenotypic variation, even in presumed simple and binary symbiotic systems, such as arthropods and their intracellular *Wolbachia*, can require a broader view of the nested network of symbiotic interactions and functions in holobionts[3]. A gut-

germline axis for microbial symbionts can also, in principle, shape evolutionary outcomes and symbiotic traits used in the biocontrol of arthropods.

Materials and methods

Fly genotype, rearing condition, and food preparation

Drosophila melanogaster y^1w^* (BDSC 1495) lines infected with *Wolbachia* strain *w*Mel were used for all the experiments. *D. melanogaster* white and yellow genetic background is extensively used in cytoplasmic incompatibility (CI) studies[7,35,36,40,46,47]. Furthermore, the *Wolbachia* strain present in this line has been effectively utilized in vector control initiatives by the World Mosquito Program[46,48]. *w*Mel uninfected lines were previously established through tetracycline treatment[35]. *Wolbachia* infection status was confirmed through PCR using Wolb_F and Wolb_R3 primers (Table S3). Flies were reared in a 12:12 h light/dark cycle at 25°C and 60-70% relative humidity. The food for both CV and GF flies had the same composition and was autoclaved. However, the autoclaved food for GF flies was maintained under sterile conditions, while the food for conventionally reared flies was maintained under non-sterile conditions. The composition for 1L media consisted of 100g yeast, 100g dextrose, 40g cornmeal, 7g agar, and 8.8 mL of 10% propionic acid dissolved in ethanol[49].

Rearing of flies to obtain mothers and fathers for hatch rate assay

Adult flies of both sexes were kept for four days for oviposition. The virgin female offspring (referred to as PGMs – paternal grandmothers) were collected on the 10th to 13th day. The PGM virgins were kept in isolation for 4-5 days to ensure virginity and to obtain moderate CI penetrance to test if germ-free treatment yields higher or lower CI penetrance[34]. Virgin PGMs were crossed with males to obtain embryos. In brief, ~30 virgin PGMs, aged 4-7 days, were

allowed to mate overnight with 10 males in an empty bottle secured with a grape plate smeared with yeast. The next morning, the grape plate was replaced by a fresh one and incubated for 30 min. The grape plate was again replaced by a new one and incubated for 1 hour to obtain 1-hour embryos. In all instances, grape plates were smeared with yeast. The embryos were processed for conventional (CV) and germ-free (GF) treatment[51]. The GF treatment was carried out as previously described[50]. Briefly, embryos were dechorionated twice using 10% bleach, followed by a single wash in 70% ethanol and three washes in PBS containing 0.1% Triton X (Fig S4). On the 2nd and 9th days after the CV and GF treatments, larvae and pupae survival were counted, respectively. On the 10th to 13th day, adult emergence was noticed. Males (referred to as fathers) less than 24 hours old were collected to perform hatch rate assay. Meanwhile, parental flies of both sexes were reared on food for 4 days to lay fertilized eggs, after which they were removed. The F1 virgin female offspring (referred to as mothers) were collected on the 10th to 13th day.

CI assays

All crosses were performed using <1-day-old males[34] and 3-day-old females in a conventional incubator under a 12:12 h light/dark cycle at 25°C with 60–70% relative humidity[16]. The matings were performed in an 8 oz polypropylene bottle and secured with a grape plate. The flies were kept overnight, and the grape plate was replaced by a fresh new grape plate. After 24 hours, the flies were cleared, and the number of embryos on the grape plate was counted (referred to as the 0-hour count). The embryos were incubated for an additional 36 hours, and the unhatched embryos were counted (referred to as 36-hour count). Any plate with less than 25 embryos was discarded. The hatching percentage was determined by calculating the percentage of embryos hatched on the 36-hour count compared to the 0-hour count. CI (incompatible) crosses were

performed between *Wolbachia*-infected males (CV+ and GF+) and *Wolbachia*-uninfected females (CV-). Compatible rescue crosses were performed between *Wolbachia*-infected males (CV+ and GF+) and *Wolbachia*-infected females (CV+). Using CV+ females for rescue experiments serves as a persistent control that ensures consistency in rescue studies[7,23,34,35,38,40] and avoids confounders by adding the extra variable of GF+ females.

Germ-free check and CFU quantification

To score the bacterial CFU in CV flies or to determine the germ-free status in GF flies, less than 24 hours old adult male flies (N=5) from each treatment were collected. However, single males from each single-pair cross were collected to assess the bacterial CFU in males from the CI assay. The flies were surface sterilized by washing twice in 70% Ethanol and once in 1x Phosphate-buffered saline (PBS). The surface sterilized flies were crushed with a sterile micro pestle, diluted in 300 uL 1xPBS, and 20 uL was used to spread onto MYPL (*Acetobacter* spp. selective media) media (Aranda-Díaz et al., 2020) and *Lactobacillus* spp. selective media MRS (Sigma, #69964, USA) plates. The MYPL media was composed of 1% D-mannitol (Sigma, #M4125, USA), 1% yeast extract (VWR, #J850, USA), 0.5% peptone (Thermo Fisher Scientific, # R451102, USA), 1% lactic acid (Sigma, #L6661, USA), 0.1% tween 80 (Thermo Fisher Scientific, #278632500, USA), adjusted to pH 7 with NaOH pellets (Spectrum Chemical, #S1301, USA), and 1.5% agar (Sigma, #A1296, USA) was added. The plates were incubated for 48 hours at 30°C and the CFU per fly was quantified using the equation:

$$CFU\ per\ fly\ = \frac{Total\ volume\ of\ homogenate\ x\ CFU\ per\ plate}{Total\ flies\ x\ Volume\ plated}$$

Microbiome reintroduction

A natural method of gut microbiome transfer based on fecal material ingestion followed a previously published protocol[51]. First, 50 adult *w*Mel+ males of random age were left in a GF vial for 7 min. Second, vials were flipped upside down for another 7 min so that the fecal material was deposited onto the plug and food surface. Finally, the resulting vials were externally surface sterilized by spraying them with ample 70% EtOH before adding the GF embryos to grow and ingest the bacteria.

RNA/DNA isolation for RT/qPCR and transcriptome

RNA was extracted and used for RT-qPCR (N=6 to 12 replicates) and RNA-Seq (N=3 replicates) from samples collected at various developmental stages for each treatment: 2-day-old larvae (N=7), late-stage pupae (N=1), and less than 24-hour-old adults (N=1). Whole body larvae/pupae/adults were frozen in liquid nitrogen and crushed with a sterile micro pestle. For *Wolbachia* density measurements, the adult abdomen was dissected and processed. RNA was extracted using 1 mL TRI Reagent (Sigma, #93289, USA) and 200 uL chloroform (Sigma, #C2432, USA). Samples were incubated for 3 min in an ice block with occasional mixing and centrifuged for 15min/12000rpm/4°C. The upper aqueous phase was transferred to an RNase-free microcentrifuge tube containing 500 uL isopropanol & 1 uL glycogen. Samples were

incubated for 10 min in an ice block with occasional mixing, and centrifuged for 10min/14000rpm/4°C. The supernatant was discarded, and the pellet was washed in 500 uL 75% EtOH followed by centrifugation for 5min/7500rpm/4°C. The pellet was air-dried inside the laminar flow hood at room temperature (RT) until it became translucent. The RNA pellet was resuspended in 30 uL of nuclease-free water and incubated at 55°C for 15 min for dissolution. Any contaminating DNA was eliminated by treating with DNA-free™ DNA Removal Kit (Thermofisher Scientific, #AM9937, USA) as per the manufacturer's instructions. RNA was confirmed DNA-free through negative PCR amplification of *rp49 Drosophila* gene. DNA-free RNA samples were then purified using the ethanol precipitation method by initially raising to 100 uL using nuclease-free water. 10 uL of 3M Sodium Acetate (Thermofisher Scientific, # R1181, USA) and 300 uL of 100% EtOH were added in the sample, mixed thoroughly & incubated at -80°C overnight. The next morning, samples were centrifuged at full speed (14000 rpm) for 30 min at 4°C and supernatant was discarded. 500 uL of freshly prepared 70% EtOH was added and centrifuged at full speed for 20 min at 4°C. The supernatant was discarded and pellet was air dried for 30 min inside the biosafety cabinet until it became transparent. Pellet was resuspended in 20 uL nuclease-free water and incubate at 55°C for 15 min to fully dissolve. The purified RNA sample was stored at -80°C until further use. cDNA was synthesized from RNA (100 ng for larvae and 1 ug for adults) with SuperScript VILO kit (Invitrogen, #11755250) and diluted 1:10 using Ambion nuclease-free water.

DNA was isolated from the non-aqueous layers from the samples used for RNA isolation using Qiagen PureGene Core Kit A kit (Qiagen, #158667, USA) following manufacturer's instructions. However, during the DNA precipitation step we added 500 uL of 100% Isopropanol and 1 uL of

glycogen to enhance the DNA recovery. qPCR was performed in 2 technical replicates using 1 uL of the diluted cDNA or DNA (10ng) and PowerTrack SYBR Green Mastermix (Applied Biosystems, #A46109) on a QuantStudio 6 Pro Real-Time PCR system using the following conditions: 50°C 2 min, 95°C 10 min, 40 cycles (15 s at 95°C , and 30 s at 56°C and 60°C for whole body and abdomen samples, respectively), 95°C 15 s, 60°C 1 min, 95°C 15 s. Gene expression of *cifA* and *cifB* (Table S3) was normalized to *groEL* and *Wolbachia* density was measured by $2^{-\Delta Ct}$ method using *groEL* relative to *rp49*. Ct values above 30 were omitted from the analysis.

Sexing of pupae

Kl-5 primers were used to sex individual pupae collected at the late stage[52]. PCR conditions used were 95°C for 2 min and 30 cycles of 95°C for 30 sec, 56°C for 30 sec, and 72°C for 1 min, final extension of 72°C for 5 min.

Transcriptome

Samples were prepared by generating a uniquely indexed library from each of the RNA samples isolated from male pupae using the Illumina Stranded Total RNA Prep with RiboZero Plus Microbiome kit (Illumina, USA) and custom *D. melanogaster* probes for the rRNA depletion. The libraries were pooled into a single pool containing an approximately equimolar amount of the samples and outsourced to the Genomic Sciences Laboratory, North Carolina State University, for sequencing using NovaSeq6000 S4 150 PE lane yielding ~25 million pairs of reads per sample on average. The raw reads were subjected to quality control using Trimgalore

v0.6.10 with a PHRED score of 20 and minimum read length of 25 bp. The cleaned reads were mapped to *D. melanogaster* reference genome (v.6.12) using STAR v2.7 to generate BAM files. The read counting was performed using the BAM files with featureCounts v2.0.6. The raw reads were rarefied using EcolUtils v0.1 with 100 permutations setting the lowest read (16M) as the threshold. The reads were then processed for downstream differentially expressed genes (DEGs) using DeSeq2 v1.42.0.

Histone staining and quantification

Less than 8 hours old males from the same population used for hatch rate assay above were dissected to collect testes in chilled 1x PBS solution and perform histone staining as described previously[7]. In brief, the testes were fixed for 30 min at RT in 4% formaldehyde prepared in 1x PBS with subsequent washing with 1x PBST solution (1x PBS + 0.3% Triton X-100) and blocking in 1% BSA for core histone at RT for an hour. Samples were incubated overnight with core histone antibody (MilliporeSigma, Cat#MABE71, USA) (1:1,000 dilution in BSA-PBST) at 4°C in rotating shaker. After washing with 1x PBST solution (1x PBS containing 0.1% Triton X-100), samples were incubated with goat anti-mouse Alexa Fluor 488 secondary antibody (Thermo Fisher Scientific, Cat#A28175, 1:500 diluted in 1x PBST) for core histone in the complete dark at RT for 4 hours. After washing in 1x PBST, samples were then mounted in vectashield DAPI-containing mounting media (Vector Laboratories, Cat#H-1200-10, USA) for imaging using Zeiss LSM 880 confocal microscope with constant exposure settings across treatment groups. The signal intensity from late canoe-stage sperm bundles that retained core histones was quantified as previously described[7], and the intensity from all stages of spermatogenesis that retained the H4ac signal was quantified and plotted in GraphPad Prism.

Protamine staining and quantification

Protamine deficiency was evaluated using chromomycin 3 (CMA3) stain as described previously[7]. In brief, mature sperm were extracted from seminal vesicles of less than 8 hours old males in chilled 1x PBS. Samples were fixed in 3:1 vol/vol methanol:acetic acid for 20 min at 4°C. Subsequently, the slide was air-dried and treated with 0.25 mg/mL of CMA3 in McIlvain's buffer, pH 7.0, with 10 mM $MgCl_2$ for 20 min. The samples were washed with 1x PBS and mounted in vectashield DAPI-containing mounting media. Imaging was performed using Zeiss LSM 880 confocal microscope. Fluorescence quantification was performed by scoring fluorescent pixels in arbitrary units (A.U.) within individual sperm heads using ImageJ. The flies were reared at 21°C instead of 25°C for this assay.

Statistical analysis

A comparison of data between two groups was performed using Kolmogorov-Smirnov tests and a Mann-Whitney U test. For more than two groups, the Kruskal Wallis test with Benjamini, Krieger & Yekutieli p-value correction was performed. A correlation test was performed using the Pearson correlation coefficient. To calculate tests and plot graphs, GraphPad Prism v10.0.0 was used.

Resource availability

Data deposition: The data reported in this paper have been deposited in Sequence Read Archive (SRA; https://www.ncbi.nlm.nih.gov/sra) (accession no. PRJNA1209084).

Acknowledgments

The authors thank the Huck Institutes Genomics Core Facility (RRID:SCR_023645) at The Pennsylvania State University for generating a uniquely indexed library from each of the RNA samples and custom *D. melanogaster* probes for the rRNA depletion. The co-authors also thank the Microscopy Core Facility (RRID:SCR_024457) for use of the Zeiss LSM 880 confocal microscope. The authors also thank Will Ludington's lab, Department of Embryology, Carnegie Institution for Science, Baltimore, MD, USA, for their expert guidance in generating germ-free flies and proofreading of the manuscript. This work was supported by The Pennsylvania State University funds to the lab of SRB.

Author contributions

M.I. and S.R.B conceived the project. M.I. and S.R.B designed the research. M.I., R.K, D.H.Z.L, M.W.B, E.L, and A.M. performed the research. M.I., R.K, E.L, and S.R.B analyzed the data. M.I. and S.R.B wrote the manuscript.

Declaration of interests

The authors declare no conflict of interest.

References

1. McFall-Ngai, M., Hadfield, M. G., Bosch, T. C. G., Carey, H. V., Domazet-Lošo, T., Douglas, A. E., Dubilier, N., Eberl, G., Fukami, T., Gilbert, S. F., Hentschel, U., King, N., Kjelleberg, S., Knoll, A. H., Kremer, N., Mazmanian, S. K., Metcalf, J. L., Nealson, K., Pierce, N. E., Rawls, J. F., Reid, A., Ruby, E. G., Rumpho, M., Sanders, J. G., Tautz, D. & Wernegreen, J. J. Animals in a bacterial world, a new imperative for the life sciences. *Proceedings of the National Academy of Sciences* **110,** 3229–3236 (2013).
2. Bordenstein, S. R. & Theis, K. R. Host Biology in Light of the Microbiome: Ten Principles of Holobionts and Hologenomes. *PLoS Biol* **13,** e1002226 (2015).
3. Bordenstein, S. R., The Holobiont Biology Network, Gilbert, M. T. P., Ginnan, N., Malacrinò, A., Martino, M. E., Bahrndorff, S., Mundra, S., Martin, M. D., Theis, K. R., Hird, S. M., Caro-Quintero, A., Sharpton, T. J., Kohl, K. D., Barnes, C. J., Eisenhofer, R., Aizpurua, O., Andersen, S. B., Brealey, J. C., Noer, C. L., Medina, M., Limborg, M. T. & Alberdi, A. The disciplinary matrix of holobiont biology. *Science (1979)* **386,** 731–732 (2024).
4. Brinker, P., Fontaine, M. C., Beukeboom, L. W. & Falcao Salles, J. Host, Symbionts, and the Microbiome: The Missing Tripartite Interaction. *Trends Microbiol* **27,** 480–488 (2019).
5. Masson, F. & Lemaitre, B. Growing Ungrowable Bacteria: Overview and Perspectives on Insect Symbiont Culturability. *Microbiol Mol Biol Rev* **84,** (2020).
6. Weinert, L. A., Araujo-Jnr, E. V., Ahmed, M. Z. & Welch, J. J. The incidence of bacterial endosymbionts in terrestrial arthropods. *Proceedings of the Royal Society B: Biological Sciences* **282,** 20150249 (2015).
7. Kaur, R., Leigh, B. A., Ritchie, I. T. & Bordenstein, S. R. The Cif proteins from Wolbachia prophage WO modify sperm genome integrity to establish cytoplasmic incompatibility. *PLoS Biol* **20,** e3001584 (2022).
8. Shropshire, J. D., Leigh, B. & Bordenstein, S. R. Symbiont-mediated cytoplasmic incompatibility: What have we learned in 50 years? *Elife* **9,** (2020).
9. Hoffmann, A. A., Turelli, M. & Harshman, L. G. Factors affecting the distribution of cytoplasmic incompatibility in Drosophila simulans. *Genetics* **126,** 933–948 (1990).
10. Shropshire, J. D., Hamant, E., Conner, W. R. & Cooper, B. S. *cifB*- transcript levels largely explain cytoplasmic incompatibility variation across divergent *Wolbachia*. *PNAS Nexus* **1,** (2022).
11. Landmann, F., Orsi, G. A., Loppin, B. & Sullivan, W. Wolbachia-Mediated Cytoplasmic Incompatibility Is Associated with Impaired Histone Deposition in the Male Pronucleus. *PLoS Pathog* **5,** e1000343 (2009).
12. Ludington, W. B. & Ja, W. W. Drosophila as a model for the gut microbiome. *PLoS Pathog* **16,** e1008398 (2020).
13. Simhadri, R. K., Fast, E. M., Guo, R., Schultz, M. J., Vaisman, N., Ortiz, L., Bybee, J., Slatko, B. E. & Frydman, H. M. The Gut Commensal Microbiome of Drosophila melanogaster Is Modified by the Endosymbiont *Wolbachia*. *mSphere* **2,** (2017).
14. Ye, Y. H., Seleznev, A., Flores, H. A., Woolfit, M. & McGraw, E. A. Gut microbiota in Drosophila melanogaster interacts with Wolbachia but does not contribute to Wolbachia -mediated antiviral protection. *J Invertebr Pathol* **143,** 18–25 (2017).

15. Shropshire, J. D., Hamant, E. & Cooper, B. S. Male Age and *Wolbachia* Dynamics: Investigating How Fast and Why Bacterial Densities and Cytoplasmic Incompatibility Strengths Vary. *mBio* **12,** (2021).
16. Kaur, R., Meier, C. J., McGraw, E. A., Hillyer, J. F. & Bordenstein, S. R. The mechanism of cytoplasmic incompatibility is conserved in Wolbachia-infected Aedes aegypti mosquitoes deployed for arbovirus control. *PLoS Biol* **22,** e3002573 (2024).
17. Ingham, P. The development of Drosophila melanogaster. *Trends in Genetics* **10,** 299 (1994).
18. Williamson, A. & Lehmann, R. GERM CELL DEVELOPMENT IN *DROSOPHILA*. *Annu Rev Cell Dev Biol* **12,** 365–391 (1996).
19. Kornberg, R. D. & Lorch, Y. Twenty-five years of the nucleosome, fundamental particle of the eukaryote chromosome. *Cell* **98,** Preprint at https://doi.org/10.1016/S0092-8674(00)81958-3 (1999)
20. Rathke, C., Baarends, W. M., Jayaramaiah-Raja, S., Bartkuhn, M., Renkawitz, R. & Renkawitz-Pohl, R. Transition from a nucleosome-based to a protamine-based chromatin configuration during spermiogenesis in *Drosophila*. *J Cell Sci* **120,** 1689–1700 (2007).
21. Akhmanova, A. S., Bindels, P. C. T., Xu, J., Miedema, K., Kremer, H., Hennig, W., Xu, J. & Hennig, W. Structure and expression of histone H3.3 genes in *Drosophila melanogaster* and *Drosophila hydei*. *Genome* **38,** 586–600 (1995).
22. Sakaguchi, A., Karachentsev, D., Seth-Pasricha, M., Druzhinina, M. & Steward, R. Functional characterization of the Drosophila Hmt4-20/Suv4-20 histone methyltransferase. *Genetics* **179,** 317–22 (2008).
23. Kaur, R., McGarry, A., Shropshire, J. D., Leigh, B. A. & Bordenstein, S. R. Prophage proteins alter long noncoding RNA and DNA of developing sperm to induce a paternal-effect lethality. *Science (1979)* **383,** 1111–1117 (2024).
24. Jayaramaiah Raja, S. & Renkawitz-Pohl, R. Replacement by *Drosophila melanogaster* Protamines and Mst77F of Histones during Chromatin Condensation in Late Spermatids and Role of Sesame in the Removal of These Proteins from the Male Pronucleus. *Mol Cell Biol* **25,** 6165–6177 (2005).
25. Eren-Ghiani, Z., Rathke, C., Theofel, I. & Renkawitz-Pohl, R. Prtl99C Acts Together with Protamines and Safeguards Male Fertility in Drosophila. *Cell Rep* **13,** 2327–2335 (2015).
26. Scholl, A., Ndoja, I., Dhakal, N., Morante, D., Ivan, A., Newman, D., Mossington, T., Clemans, C., Surapaneni, S., Powers, M. & Jiang, L. The Osiris family genes function as novel regulators of the tube maturation process in the Drosophila trachea. *PLoS Genet* **19,** e1010571 (2023).
27. Ikeda, T., Ishikawa, H. & Sasaki, T. Infection density of Wolbachia and level of cytoplasmic incompatibility in the Mediterranean flour moth, Ephestia kuehniella. *J Invertebr Pathol* **84,** 1–5 (2003).
28. Ritchie, I. T., Needles, K. T., Leigh, B. A., Kaur, R. & Bordenstein, S. R. Transgenic cytoplasmic incompatibility persists across age and temperature variation in Drosophila melanogaster. *iScience* **25,** 105327 (2022).
29. Bordenstein, S. R., Uy, J. J. & Werren, J. H. Host Genotype Determines Cytoplasmic Incompatibility Type in the Haplodiploid Genus Nasonia. *Genetics* **164,** 223–233 (2003).
30. Aranda-Díaz, A., Obadia, B., Dodge, R., Thomsen, T., Hallberg, Z. F., Güvener, Z. T., Ludington, W. B. & Huang, K. C. Bacterial interspecies interactions modulate pH-mediated antibiotic tolerance. *Elife* **9,** (2020).

31. Newell, P. D. & Douglas, A. E. Interspecies Interactions Determine the Impact of the Gut Microbiota on Nutrient Allocation in Drosophila melanogaster. *Appl Environ Microbiol* **80,** 788–796 (2014).
32. Sommer, A. J. & Newell, P. D. Metabolic Basis for Mutualism between Gut Bacteria and Its Impact on the *Drosophila melanogaster* Host. *Appl Environ Microbiol* **85,** (2019).
33. Chaston, J. M., Dobson, A. J., Newell, P. D. & Douglas, A. E. Host genetic control of the microbiota mediates the Drosophila nutritional phenotype. *Appl Environ Microbiol* **82,** (2016).
34. Layton, E. M., On, J., Perlmutter, J. I., Bordenstein, S. R. & Shropshire, J. D. Paternal Grandmother Age Affects the Strength of *Wolbachia* -Induced Cytoplasmic Incompatibility in Drosophila melanogaster. *mBio* **10,** (2019).
35. LePage, D. P., Metcalf, J. A., Bordenstein, S. R., On, J., Perlmutter, J. I., Shropshire, J. D., Layton, E. M., Funkhouser-Jones, L. J., Beckmann, J. F. & Bordenstein, S. R. Prophage WO genes recapitulate and enhance Wolbachia-induced cytoplasmic incompatibility. *Nature* **543,** 243–247 (2017).
36. Bourtzis, K., Nirgianaki, A., Markakis, G. & Savakis, C. Wolbachia Infection and Cytoplasmic Incompatibility in Drosophila Species. *Genetics* **144,** 1063–1073 (1996).
37. Cooper, B. S., Ginsberg, P. S., Turelli, M. & Matute, D. R. Wolbachia in the *Drosophila yakuba* Complex: Pervasive Frequency Variation and Weak Cytoplasmic Incompatibility, but No Apparent Effect on Reproductive Isolation. *Genetics* **205,** 333–351 (2017).
38. Shropshire, J. D., On, J., Layton, E. M., Zhou, H. & Bordenstein, S. R. One prophage WO gene rescues cytoplasmic incompatibility in *Drosophila melanogaster*. *Proceedings of the National Academy of Sciences* **115,** 4987–4991 (2018).
39. Reynolds, K. T. & Hoffmann, A. A. Male age, host effects and the weak expression or non-expression of cytoplasmic incompatibility in Drosophila strains infected by maternally transmitted Wolbachia. *Genet Res* **80,** (2002).
40. Yamada, R., Floate, K. D., Riegler, M. & O'Neill, S. L. Male Development Time Influences the Strength of Wolbachia-Induced Cytoplasmic Incompatibility Expression in *Drosophila melanogaster*. *Genetics* **177,** 801–808 (2007).
41. Numajiri, Y., Kondo, N. I., Toquenaga, Y. & Kageyama, D. Intraspecies variation in cytoplasmic incompatibility intensity in the bean beetle Callosobruchus analis. *Evol Ecol* **38,** 861–870 (2024).
42. Sasaki, T., Kubo, T. & Ishikawa, H. Interspecific Transfer of Wolbachia Between Two Lepidopteran Insects Expressing Cytoplasmic Incompatibility: A Wolbachia Variant Naturally Infecting *Cadra cautella* Causes Male Killing in *Ephestia kuehniella*. *Genetics* **162,** 1313–1319 (2002).
43. Suwanchaisri, K., Roddee, J. & Wangkeeree, J. Wolbachia Transinfection and Effect on the Biological Traits of Matsumuratettix hiroglyphicus (Matsumura), the Leafhopper Vector of Sugarcane White Leaf Disease. *Agriculture* **14,** 1236 (2024).
44. Hughes, G. L., Dodson, B. L., Johnson, R. M., Murdock, C. C., Tsujimoto, H., Suzuki, Y., Patt, A. A., Cui, L., Nossa, C. W., Barry, R. M., Sakamoto, J. M., Hornett, E. A. & Rasgon, J. L. Native microbiome impedes vertical transmission of *Wolbachia* in *Anopheles* mosquitoes. *Proceedings of the National Academy of Sciences* **111,** 12498–12503 (2014).

45. Detcharoen, M., Jiggins, F. M., Schlick-Steiner, B. C. & Steiner, F. M. Wolbachia endosymbiotic bacteria alter the gut microbiome in the fly Drosophila nigrosparsa. *J Invertebr Pathol* **198,** 107915 (2023).
46. Walker, T., Johnson, P. H., Moreira, L. A., Iturbe-Ormaetxe, I., Frentiu, F. D., McMeniman, C. J., Leong, Y. S., Dong, Y., Axford, J., Kriesner, P., Lloyd, A. L., Ritchie, S. A., O'Neill, S. L. & Hoffmann, A. A. The wMel Wolbachia strain blocks dengue and invades caged Aedes aegypti populations. *Nature* **476,** (2011).
47. Blagrove, M. S. C., Arias-Goeta, C., Failloux, A. B. & Sinkins, S. P. Wolbachia strain wMel induces cytoplasmic incompatibility and blocks dengue transmission in Aedes albopictus. *Proc Natl Acad Sci U S A* **109,** (2012).
48. O'Neill, S. L. in *Adv Exp Med Biol* **1062,** (2018).
49. Suito, T., Nagao, K., Juni, N., Hara, Y., Sokabe, T., Atomi, H. & Umeda, M. Regulation of thermoregulatory behavior by commensal bacteria in *Drosophila*. *Biosci Biotechnol Biochem* **86,** 1060–1070 (2022).
50. Koyle, M. L., Veloz, M., Judd, A. M., Wong, A. C.-N., Newell, P. D., Douglas, A. E. & Chaston, J. M. Rearing the Fruit Fly Drosophila melanogaster Under Axenic and Gnotobiotic Conditions. *Journal of Visualized Experiments* (2016). doi:10.3791/54219
51. Chandler, J. A., Innocent, L. V., Martinez, D. J., Huang, I. L., Yang, J. L., Eisen, M. B. & Ludington, W. B. Microbiome-by-ethanol interactions impact Drosophila melanogaster fitness, physiology, and behavior. *iScience* **25,** 104000 (2022).
52. Lott, S. E., Villalta, J. E., Schroth, G. P., Luo, S., Tonkin, L. A. & Eisen, M. B. Noncanonical Compensation of Zygotic X Transcription in Early Drosophila melanogaster Development Revealed through Single-Embryo RNA-Seq. *PLoS Biol* **9,** e1000590 (2011).

Fig 1. CI penetrance is stronger in germ-free males and links with host regulation of histone, protamine, and male-specific transcripts. (A) Schematic representation of the fly lines showing (from left to right): complete symbiont community, gut microbiome only, endosymbiont (*Wolbachia*) only, and symbiont-free. (B) Germ-free males with *Wolbachia* (GF+) induce significantly higher incompatibility (dark pink) than conventional (CV+) males. CI is a metric for embryonic viability that is measured by the percentage of embryos that develop into larvae. Compatible crosses (grey bars) with normal embryonic hatching percentages are controls that express either no CI or rescue of CI. P-values were calculated based on a Kruskal-Wallis test followed by Benjamini, Krieger, and Yekutieli multiple correction test. (C) GF+ males with a native microbiome reintroduced ($GF+_M$) recapitulate the CI strength similar to CV+ males. (D) Comparative transcriptomic analysis of GF+ vs. CV+ male pupae and GF- vs. CV- male pupae revealed significant differentially expressed genes narrowed here to 37 genes expressing histone, protamine, and male-specific transcripts (MSTs). Significant differences are highlighted with a black colored asterisk (*). Notably, the histone-related genes genes (red) were upregulated, while protamine (green) and MST (blue) genes were downregulated. Log2 fold change was calculated using DESeq2, and its default parameters; Walt test and Benjamini-Hochberg procedure were used to calculate p and adjusted p-values. The asterisk *, **, and *** represent adjusted p-values less than 0.05, 0.005, and 0.0005, respectively.

Fig 2. CI defects in the histone-to-protamine transition occur in germ-free and conventional males. (A) During *Drosophila melanogaster* sperm development, chromatin is initially packaged with histones. In the late canoe stage, histones are replaced by protamines and protamine-like proteins, facilitating tight chromatin condensation within the sperm head. We

tested if there is variation in the histone-protamine transition using testes (N = ~10) from <8-hour-old virgin males of GF-, GF+, CV-, and CV+ lines were dissected and (B) immunostained to visualize and quantify histone abundance (magenta) in late-canoe elongating spermatids. DAPI stain (grey) was used to label spermatid nuclei, and (C) CMA3 stained for protamine deficiency. Signal intensity from each stained spermatid with signal was quantified in ImageJ and graphed. (B) GF+ and CV+ late canoe spermatids both significantly retain histones compared to their negative counterparts GF- and CV-, respectively. (C) GF+ and CV+ mature sperm have enhanced CMA3 intensity, consistent with protamine deficiency levels compared to GF- and CV- negative controls, respectively. Vertical bars represent the median, and error bars represent the standard deviation. P-values are calculated using the Mann-Whitney U test in Prism.

Fig 3. *Wolbachia* density and transcriptional activity vary with host developmental stage and microbiome status. (A) Relative to CV+ males, *Wolbachia* densities were significantly lower in the GF+ adult males and (B) similar in GF+ larvae using sigle copy genes of the endosymbiont (*groEL*) and host (*rp49*). (D-F) *cifA* and *cifB* gene expression in adults and larvae were similar between CV+ and GF+ males, suggesting that the neither *Wolbachia* density nor *cif* gene expression underpin exacerbated CI in GF+ flies. The p-values are shown for the non-parametric Kolmogorov-Smirnov [and Mann-Whitney U] tests. (G) *Wolbachia* transcriptomes across development reveal that *Wolbachia* are transcriptionally more active in GF+ compared to CV+, particularly in the larval stage. Among the differentially-expressed genes, the most common types of transcripts were hypothetical and microbial interactions, such as transcripts with ankyrin repeat domains.

Fig 4. Holobionts with *Wolbachia* have higher colony forming units (CFUs) of gut bacteria. (A) Homogenates of less than one day old CV- (white circles) and CV+ males (orange circles) (N=5) in triplicates were spread on MRS and MYPL plates. (B) *Wolbachia* infection (CV+) significantly increased the CFU load of *Acetobacter spp*. and *Lactobacillus spp*., suggesting a positive interaction between the endosymbiont and the microbiome. The p-values are calculated with a Mann-Whitney U test. (C) The CFU of *Acetobacter* spp. and *Lactobacillus* spp. in CV- (data points filled in white) and CV+ (data points with filled in orange color) males have a significant positive correlation. All flies were surface sterilized to avoid transient bacteria residing on the fly surface. A CFU count below 500 is typical in most flies, as young flies (<1 day old) have not yet developed a fully established gut microbiome.

Fig 5. The fitness impacts of *Wolbachia* and gut microbiome are independent and developmentally staged, and microbiome reintroduction into germ-free flies restores fly fitness. (A) The extracellular microbiome and *Wolbachia* exert independent and positive effects on embryo-to-larval survival, as calcuated by the number of surving larvae divided by the number of emryos laid for CV+ vs. CV- and GF+ vs. GF-. (B) The extracellular microbiome is beneficial to larval-to-pupal survival, while *Wolbachia* imposes a fitness cost in a microbiome-independent manner. (D) Similarly, *Wolbachia* lower pupal-to-adult survival percentage in a microbiome-independent manner. (D) The overall trend from embry-to-adult shows GF+ flies consistently performing weker comapred to CV+. The top green bar represents the positive fitness effect of the microbiome on the host, while the green and red lines at the bottom indicate the positive and negative effects, respectively, of *Wolbachia* on the host. (E) When the

conventional microbiome was re-introduced into GF+ flies through fecal-to-oral transmission, the egg-to-adult survival of the recipient flies (GF_M+) significantly increased to the same level as that of CV+ flies. Each circle represents a family, and color denotes genotype status: orange bar (CV), blue bar (GF), open circle (no *Wolbachia*), and filled cirlce (*Wolbachia*). The p-values were calculated with Kruskal-Wallis test followed by Benjamini, Krieger, and Yekutieli multiple correction test.

SUPPORTING INFORMATION

S1 Fig. Confirmation of gut microbiome absence and presence by colony forming units (CFUs) in GF and CV lines. The germ-free status of the GF-/+ lines was confirmed by the absence of colonies when 20uL of fly homogenate were plated on to MYPL and MRS plates. The conventionally-reared positive control lines had ample colonies with colony number significantly elevated in CV+ relative to CV- flies.

S2 Fig. The top misregulated transcripts link with reproductive, chitin, cuticle, and sensory development. The diffrentially-expressed transcripts that were significant (adjusted $p<0.05$) are shown for (A) GF+ vs CV+ male pupae and (B) GF- vs CV- male puape.

S3 Fig. Copy number of host *rp49* in CV+ and GF+ are comparable. (A) Standard curves for the absolute quantification of *rp49* were generated using a log10 dilution series of known amounts of PCR product amplified from a larger region of the same *rp49* gene (404 bp). PCR amplification was performed using primers listed in Table S1 at a concentration of 0.4 µM. The cycling conditions were as follows: 30 cycles of 95°C for 15 seconds, 60°C for 30 seconds, and 72°C for 30 seconds. The PCR products were purified using the Monarch DNA Purification Kit (NEB) and their concentrations were measured using a NanoDrop One spectrophotometer. The number of *rp49* copies was calculated using the following formula: Number of DNA copies = (amount of DNA in ng * 6.022 x 10^23) / length of amplicon in bp x 10^9 x 660). Standard curve was plotting using Design & Analysis Software v2.8.0 (B) Mann Whitney U test of the CV+ and GF+ shows that the absolute count of CV+ and GF+ *rp49* gene in their abdomen are similar.

S4 Fig. Dechorination of *Drosophila melanogaster* embryos. The germ-free treatment followed the standard procedure of bleaching fertilized embryos. Briefly, CV- and CV+ females were allowed to oviposit overnight on a grape plate smeared with yeast. The next morning, the grape plates were replaced with fresh ones smeared with yeast, and the flies were allowed to oviposit for 30 minutes. This was followed by another replacement with a fresh grape plate smeared with yeast, where the flies oviposited for an additional hour to collect 1-hour embryos. The collected embryos were transferred to a petri dish and approximately half was transferred into a cell strainer. These embryos were bleached twice in 10% bleach for 2.5 minutes each, followed by a single wash in 70% ethanol for 30 seconds and three quick washes in PBS containing 0.1% Triton X for 10 seconds each. The dechorionated eggs were carefully counted under a stereomicroscope and then placed on a germ-free grape plate or a germ-free food vial before being incubated under sterile conditions.

S1 Table: Genetic comparison between CV- and CV+ lines

S2 Table: Differentially-expressed histone, protamine, and MST transcripts in male pupae.

S3 Table: Primers used for measuring *Wolbachia* density, sex of pupae, and *cifA* and *cifB* expression.

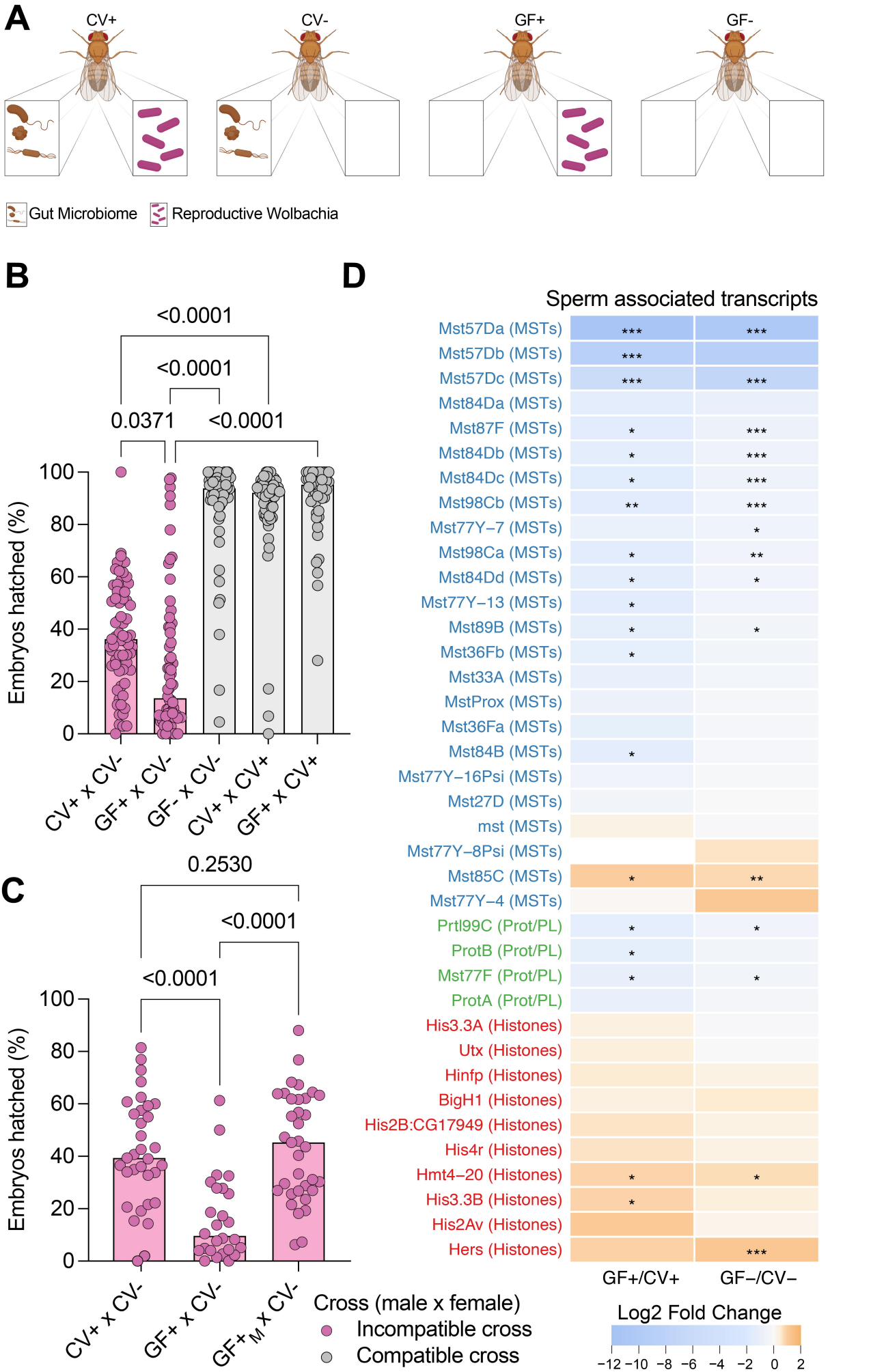
A
CV+
CV-
GF+
GF-
Gut Microbiome
Reproductive Wolbachia
B
<0.0001
<0.0001
0.0371
<0.0001
Embryos hatched (%)
100
80
60
40
20
0
CV+ x CV-
GF+ x CV-
GF- x CV-
CV+ x CV+
GF+ x CV+
C
0.2530
<0.0001
<0.0001
Embryos hatched (%)
100
80
60
40
20
0
CV+ x CV-
GF+ x CV-
GF+M x CV-
Cross (male x female)
Incompatible cross
Compatible cross
D
Sperm associated transcripts
Mst57Da (MSTs) *** ***
Mst57Db (MSTs) ***
Mst57Dc (MSTs) *** ***
Mst84Da (MSTs)
Mst87F (MSTs) * ***
Mst84Db (MSTs) * ***
Mst84Dc (MSTs) * ***
Mst98Cb (MSTs) ** ***
Mst77Y−7 (MSTs) *
Mst98Ca (MSTs) * **
Mst84Dd (MSTs) * *
Mst77Y−13 (MSTs) *
Mst89B (MSTs) * *
Mst36Fb (MSTs) *
Mst33A (MSTs)
MstProx (MSTs)
Mst36Fa (MSTs)
Mst84B (MSTs) *
Mst77Y−16Psi (MSTs)
Mst27D (MSTs)
mst (MSTs)
Mst77Y−8Psi (MSTs)
Mst85C (MSTs) * **
Mst77Y−4 (MSTs)
Prtl99C (Prot/PL) * *
ProtB (Prot/PL) *
Mst77F (Prot/PL) * *
ProtA (Prot/PL)
His3.3A (Histones)
Utx (Histones)
Hinfp (Histones)
BigH1 (Histones)
His2B:CG17949 (Histones)
His4r (Histones)
Hmt4−20 (Histones) * *
His3.3B (Histones) *
His2Av (Histones)
Hers (Histones) ***
GF+/CV+
GF−/CV−
Log2 Fold Change
−12 −10 −8 −6 −4 −2 0 2

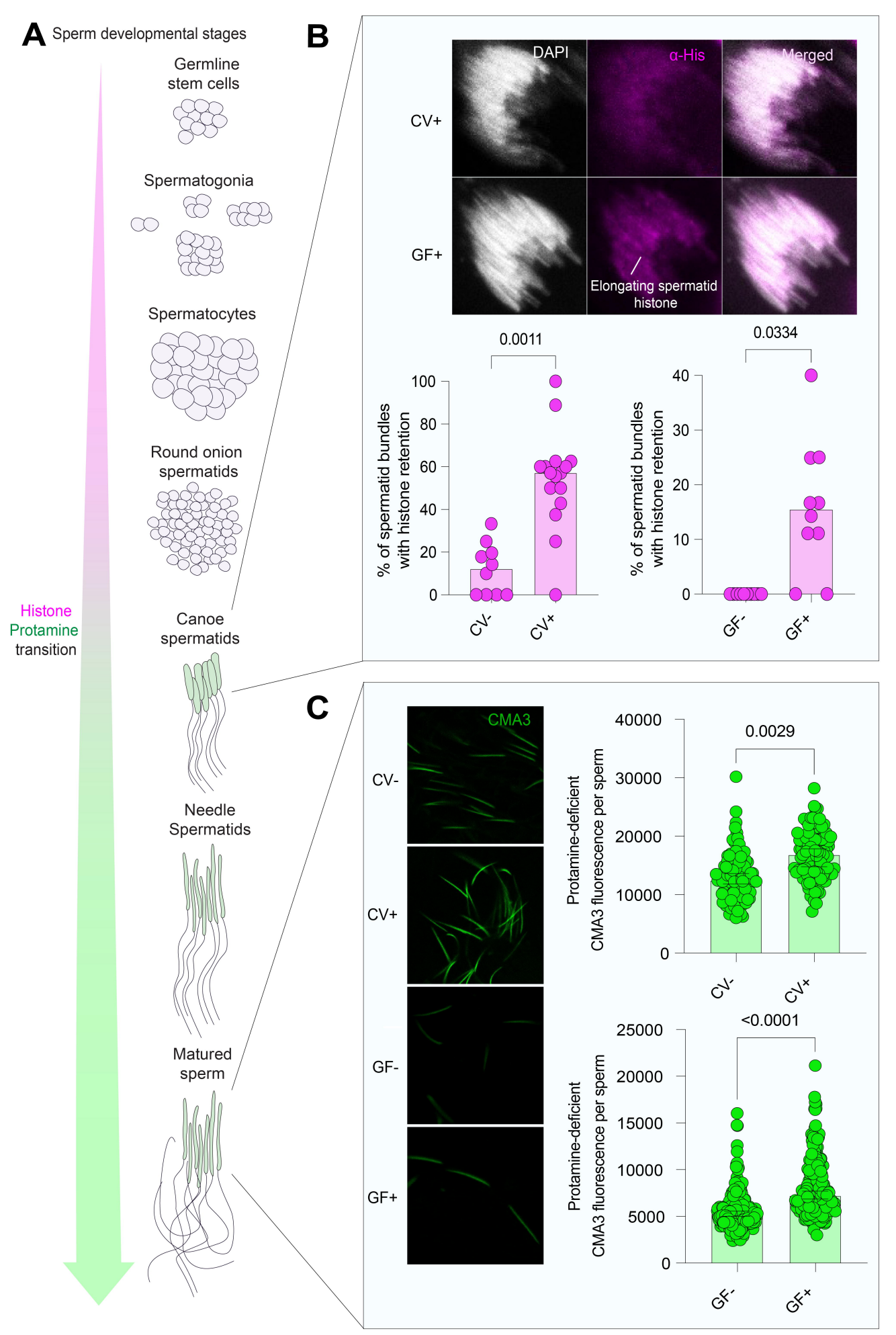
A
Sperm developmental stages
Germline stem cells
Spermatogonia
Spermatocytes
Round onion spermatids
Canoe spermatids
Needle Spermatids
Matured sperm
Histone
Protamine
transition
B
DAPI
α-His
Merged
CV+
GF+
Elongating spermatid histone
0.0011
% of spermatid bundles with histone retention
CV-
CV+
0.0334
GF-
GF+
C
CMA3
CV-
CV+
GF-
GF+
Protamine-deficient CMA3 fluorescence per sperm
0.0029
<0.0001

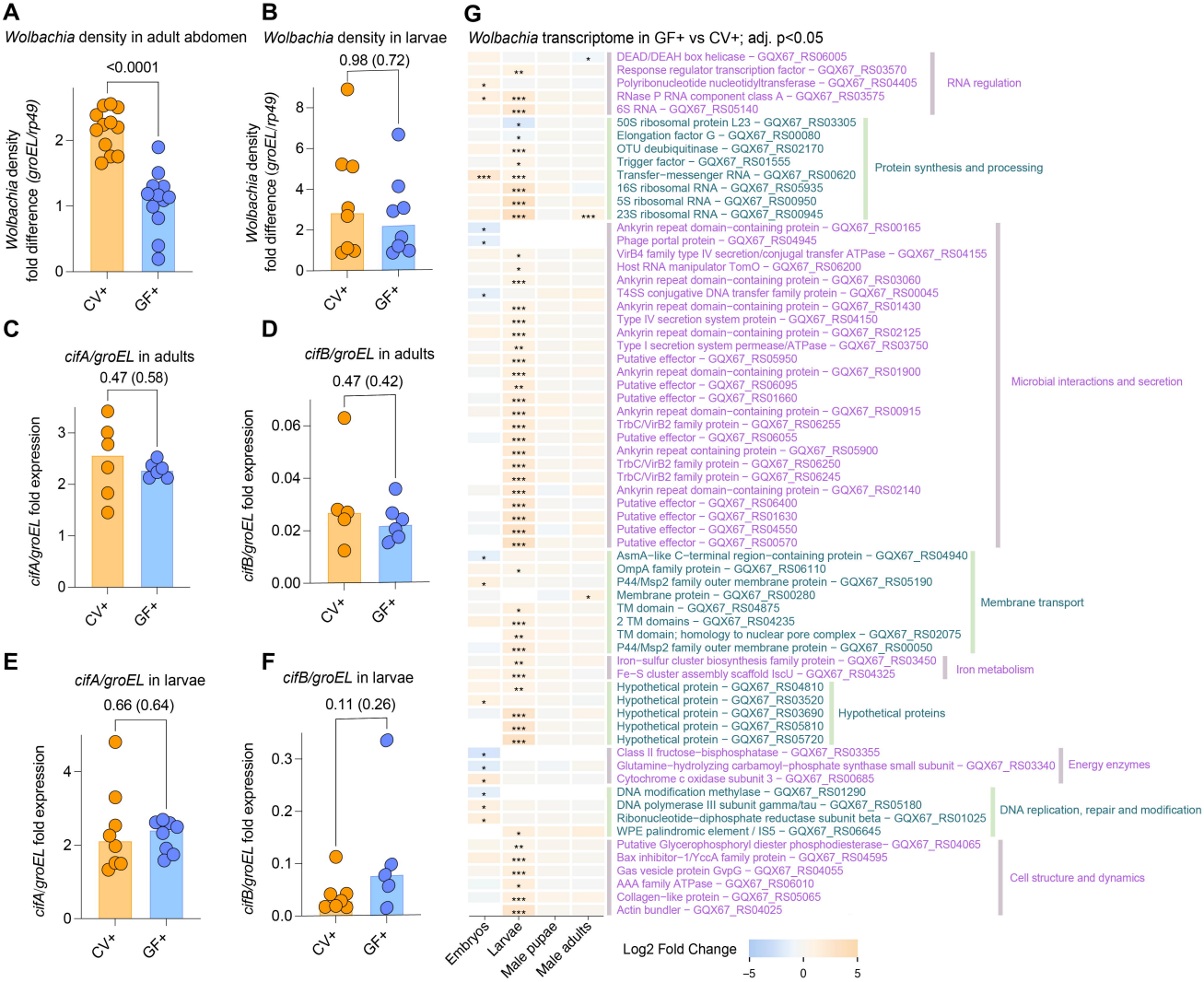
A
Wolbachia density in adult abdomen
<0.0001
Wolbachia density fold difference (groEL/rp49)
CV+
GF+
B
Wolbachia density in larvae
0.98 (0.72)
Wolbachia density fold difference (groEL/rp49)
CV+
GF+
C
cifA/groEL in adults
0.47 (0.58)
cifA/groEL fold expression
CV+
GF+
D
cifB/groEL in adults
0.47 (0.42)
cifB/groEL fold expression
CV+
GF+
E
cifA/groEL in larvae
0.66 (0.64)
cifA/groEL fold expression
CV+
GF+
F
cifB/groEL in larvae
0.11 (0.26)
cifB/groEL fold expression
CV+
GF+
G
Wolbachia transcriptome in GF+ vs CV+; adj. p<0.05
DEAD/DEAH box helicase − GQX67_RS06005
Response regulator transcription factor − GQX67_RS03570
Polyribonucleotide nucleotidyltransferase − GQX67_RS04405
RNase P RNA component class A − GQX67_RS03575
6S RNA − GQX67_RS05140
RNA regulation
50S ribosomal protein L23 − GQX67_RS03305
Elongation factor G − GQX67_RS00080
OTU deubiquitinase − GQX67_RS02170
Trigger factor − GQX67_RS01555
Transfer−messenger RNA − GQX67_RS00620
16S ribosomal RNA − GQX67_RS05935
5S ribosomal RNA − GQX67_RS00950
23S ribosomal RNA − GQX67_RS00945
Protein synthesis and processing
Ankyrin repeat domain−containing protein − GQX67_RS00165
Phage portal protein − GQX67_RS04945
VirB4 family type IV secretion/conjugal transfer ATPase − GQX67_RS04155
Host RNA manipulator TomO − GQX67_RS06200
Ankyrin repeat domain−containing protein − GQX67_RS03060
T4SS conjugative DNA transfer family protein − GQX67_RS00045
Ankyrin repeat domain−containing protein − GQX67_RS01430
Type IV secretion system protein − GQX67_RS04150
Ankyrin repeat domain−containing protein − GQX67_RS02125
Type I secretion system permease/ATPase − GQX67_RS03750
Putative effector − GQX67_RS05950
Ankyrin repeat domain−containing protein − GQX67_RS01900
Putative effector − GQX67_RS06095
Putative effector − GQX67_RS01660
Ankyrin repeat domain−containing protein − GQX67_RS00915
TrbC/VirB2 family protein − GQX67_RS06255
Putative effector − GQX67_RS06055
Ankyrin repeat containing protein − GQX67_RS05900
TrbC/VirB2 family protein − GQX67_RS06250
TrbC/VirB2 family protein − GQX67_RS06245
Ankyrin repeat domain−containing protein − GQX67_RS02140
Putative effector − GQX67_RS06400
Putative effector − GQX67_RS01630
Putative effector − GQX67_RS04550
Putative effector − GQX67_RS00570
Microbial interactions and secretion
AsmA−like C−terminal region−containing protein − GQX67_RS04940
OmpA family protein − GQX67_RS06110
P44/Msp2 family outer membrane protein − GQX67_RS05190
Membrane protein − GQX67_RS00280
TM domain − GQX67_RS04875
2 TM domains − GQX67_RS04235
TM domain; homology to nuclear pore complex − GQX67_RS02075
P44/Msp2 family outer membrane protein − GQX67_RS00050
Membrane transport
Iron−sulfur cluster biosynthesis family protein − GQX67_RS03450
Fe−S cluster assembly scaffold IscU − GQX67_RS04325
Iron metabolism
Hypothetical protein − GQX67_RS04810
Hypothetical protein − GQX67_RS03520
Hypothetical protein − GQX67_RS03690
Hypothetical protein − GQX67_RS05810
Hypothetical protein − GQX67_RS05720
Hypothetical proteins
Class II fructose−bisphosphatase − GQX67_RS03355
Glutamine−hydrolyzing carbamoyl−phosphate synthase small subunit − GQX67_RS03340
Cytochrome c oxidase subunit 3 − GQX67_RS00685
Energy enzymes
DNA modification methylase − GQX67_RS01290
DNA polymerase III subunit gamma/tau − GQX67_RS05180
Ribonucleotide−diphosphate reductase subunit beta − GQX67_RS01025
WPE palindromic element / IS5 − GQX67_RS06645
DNA replication, repair and modification
Putative Glycerophosphoryl diester phosphodiesterase− GQX67_RS04065
Bax inhibitor−1/YccA family protein − GQX67_RS04595
Gas vesicle protein GvpG − GQX67_RS04055
AAA family ATPase − GQX67_RS06010
Collagen−like protein − GQX67_RS05065
Actin bundler − GQX67_RS04025
Cell structure and dynamics
Embryos
Larvae
Male pupae
Male adults
Log2 Fold Change
−5
0
5

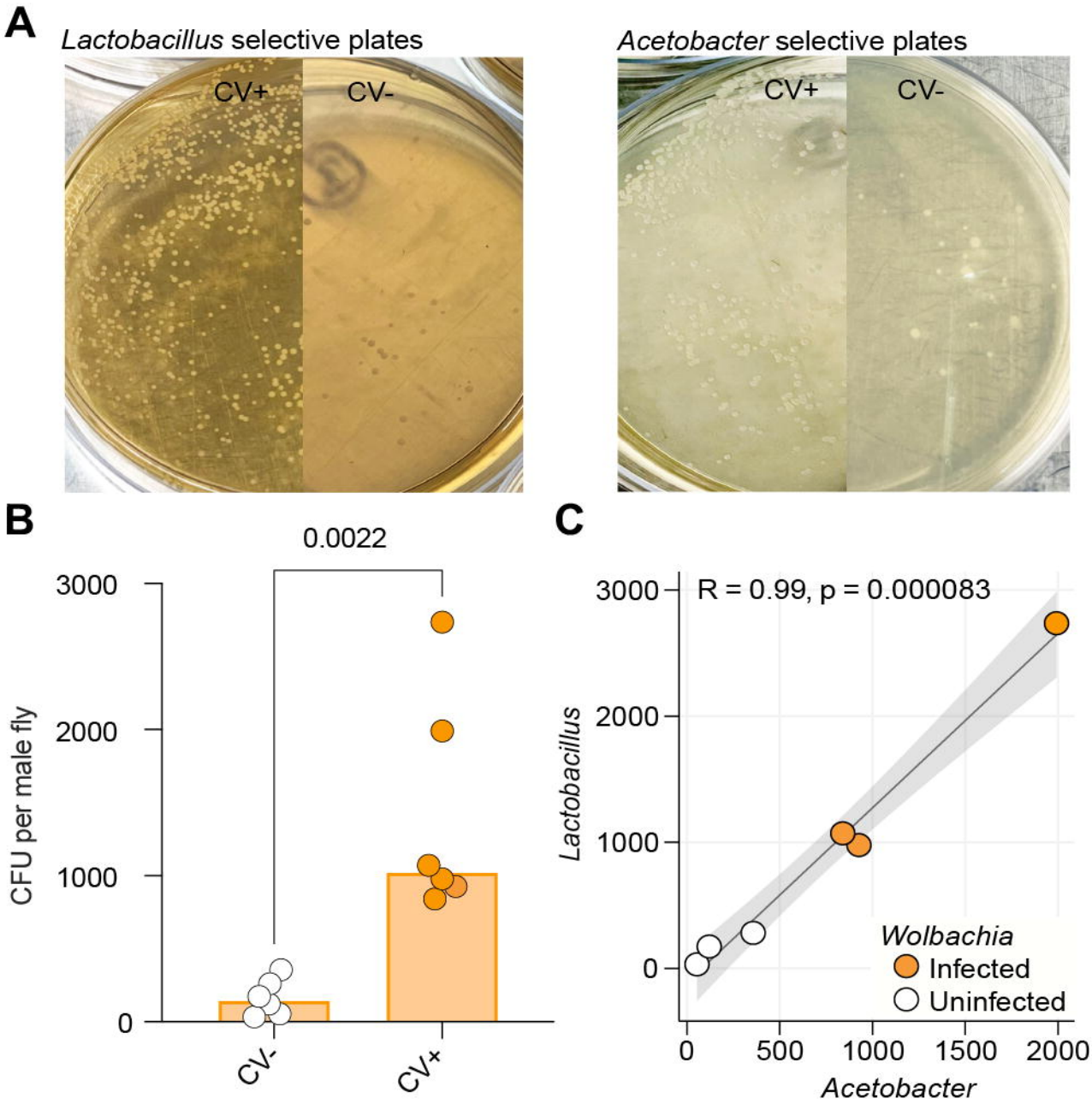
A
Lactobacillus selective plates
CV+
CV-
Acetobacter selective plates
CV+
CV-
B
0.0022
3000
2000
1000
0
CFU per male fly
CV-
CV+
C
R = 0.99, p = 0.000083
3000
2000
1000
0
Lactobacillus
0
500
1000
1500
2000
Acetobacter
Wolbachia
Infected
Uninfected

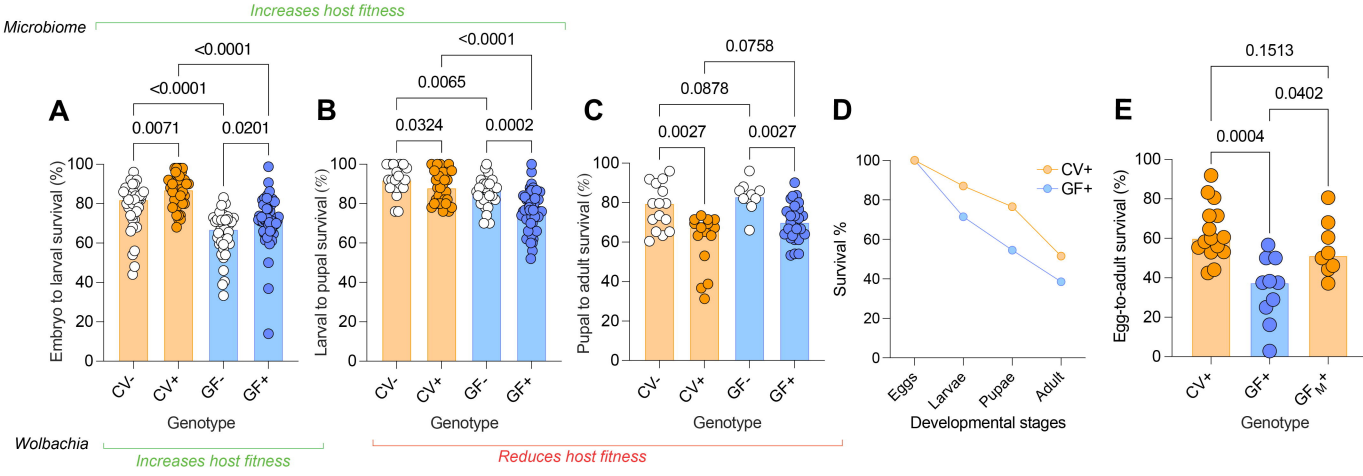
Microbiome
Increases host fitness
A
<0.0001
<0.0001
0.0071
0.0201
Embryo to larval survival (%)
CV-
CV+
GF-
GF+
Genotype
B
<0.0001
0.0065
0.0324
0.0002
Larval to pupal survival (%)
C
0.0758
0.0878
0.0027
0.0027
Pupal to adult survival (%)
D
CV+
GF+
Survival %
Eggs
Larvae
Pupae
Adult
Developmental stages
E
0.1513
0.0402
0.0004
Egg-to-adult survival (%)
GF_M+
Wolbachia
Increases host fitness
Reduces host fitness